Published for SISSA by Springer

Received: *September 13, 2012*
Revised: *November 21, 2012*
Accepted: *December 29, 2012*
Published: *February 1, 2013*

# MSSM electroweak baryogenesis and LHC data

**M. Carena,**[a] **G. Nardini,**[b] **M. Quirós**[c] **and C.E.M. Wagner**[d,e]

[a] *Theoretical Physics Department, Fermilab, P.O. Box 500, Batavia, IL 60510, U.S.A.*
[b] *Fakultät für Physik, Universität Bielefeld, Universitätsstrasse 25, D-33615 Bielefeld, Germany*
[c] *IFAE and Institució Catalana de Recerca i Estudis Avançats (ICREA), Universitat Autònoma de Barcelona, 08193 Bellaterra, Barcelona, Spain*
[d] *HEP Division, Argonne National Laboratory, 9700 S. Cass Ave., Argonne, IL 60439, U.S.A.*
[e] *EFI, KICP and Physics Department, University of Chicago, 5640 S. Ellis Ave., Chicago, IL 60637, U.S.A.*

*E-mail:* carena@fnal.gov, germano@physik.uni-bielefeld.de, quiros@ifae.es, cwagner@hep.anl.gov

Abstract: Electroweak baryogenesis is an attractive scenario for the generation of the baryon asymmetry of the universe as its realization depends on the presence at the weak scale of new particles which may be searched for at high energy colliders. In the MSSM it may only be realized in the presence of light stops, and with moderate or small mixing between the left- and right-handed components. Consistency with the observed Higgs mass around 125 GeV demands the heavier stop mass to be much larger than the weak scale. Moreover the lighter stop leads to an increase of the gluon-gluon fusion Higgs production cross section which seems to be in contradiction with indications from current LHC data. We show that this tension may be considerably relaxed in the presence of a light neutralino with a mass lower than about 60 GeV, satisfying all present experimental constraints. In such a case the Higgs may have a significant invisible decay width and the stop decays through a three or four body decay channel, including a bottom quark and the lightest neutralino in the final state. All these properties make this scenario testable at a high luminosity LHC.

Keywords: Supersymmetry Phenomenology

ArXiv ePrint: 1207.6330



doi:10.1007/JHEP02(2013)001

JHEP02(2013)001

## Contents



## 1 Introduction

The origin of the baryon asymmetry is one of the most important open questions in particle physics and cosmology. The generation of baryon asymmetry requires $CP$ and baryon number violation, as well as non-equilibrium processes [1]. In the Standard Model (SM) $CP$ violation is present in the CKM fermion mixing, baryon number violation is associated with non-perturbative sphaleron processes and departure from equilibrium may occur at the electroweak phase transition at finite temperature, below which the Higgs acquires a vacuum expectation value (VEV). For this to happen a strongly first order phase transition should take place in which the vacuum expectation value of the Higgs $v(T_n)$ at the nucleation temperature $T_n$ fulfills the condition $v(T_n)/T_n \gtrsim 1$ [2–6]. However for Higgs masses in the allowed range the electroweak phase transition in the SM is a cross-over, and therefore the mechanism of Electroweak Baryogenesis (EWBG) is not realized [7–10]. Moreover even if the phase transition were strong enough, the SM CP-violating sources are too weak to lead to the observed baryon asymmetry [11–14].

The realization of the EWBG scenario demands new physics at the weak scale. Since new physics at this scale is also required for a natural realization of the Higgs mechanism it is natural to concentrate on beyond the SM scenarios that fulfill this property. In particular the Minimal Supersymmetric extension of the Standard Model (MSSM) is a well motivated one, not only based on symmetry arguments but also leading to the cancellation of quadratic divergences of the Higgs mass parameter, to the unification of couplings at high energies, and to a natural Dark Matter (DM) candidate. Moreover it has been shown [15–41] that in the presence of a light top squark (stop), with mass lower than about 120 GeV, and Higgs masses below about 127 GeV (see ref. [41]) the phase transition can be sufficiently strong as to allow the realization of this scenario. New CP-violating sources may be



JHEP02(2013)001

achieved associated with the light charginos and neutralinos mass parameters. Therefore all these properties make the MSSM electroweak baryogenesis scenario testable at current experiments, in particular in view of the recent observation of a Higgs-like resonance with mass close to 125 GeV at both LHC experiments [42–48].

The Higgs boson mass in the MSSM depends on loop effects, mainly associated with the stops. It depends logarithmically on the stop masses, and quadratically and quartically on the mixing parameter in the stop sector. For a light stop as the one required for baryogenesis, a Higgs boson mass $m_h$ above 115 GeV, consistent with the LEP bounds, may only be obtained for a large mixing parameter or for a large value of the heaviest stop [49]. The large mixing parameter necessary to raise the Higgs mass suppresses the coupling of the lightest stop to the Higgs and prevents it to have a large effect on the phase transition. Therefore, for EWBG to be realized, the heaviest stop mass must be much larger than 1 TeV and the stop mixing parameter must be moderate, with values lower than a half of the heaviest stop mass [49].

A light stop with small mixing and relevant coupling to the Higgs tends to enhance by tens of percent, or even factors of a few, the SM-like Higgs gluon fusion production rate, and somewhat reduces the decay width into photons, with respect to the SM [50, 51]. Therefore in the decoupling limit, for large values of the CP-odd Higgs mass, the enhancement of $\sigma(gg \to h \to \gamma\gamma)$ is somewhat smaller than the associated enhancement of $\sigma(gg \to h \to WW, ZZ)$. As it has recently been pointed out by two different groups [52, 53] such properties are in tension with the current Higgs search data at LHC [42–48].

In this article we reanalyze the Higgs mass constraints and we will show that the tension with data may be significantly reduced in the presence of a light neutralino, with a mass lower than 60 GeV. We shall show that such scenario is consistent with all present experimental bounds, in particular with the stop and $Z$-boson decay constraints. In this case the Higgs may have a significant invisible decay width which can compensate the otherwise enhanced $WW$- and $ZZ$-production rates. In the 125 GeV Higgs-mass region the latter rates may be close to the ones associated with a SM Higgs, and therefore consistent with current experimental bounds.

This paper is organized as follows. In section 2 we review the Light Stop Scenario (LSS) and the conditions for EWBG. In section 3 we review the constraints from stop and Higgs searches and study the phenomenological consequences of a light neutralino. In section 4 we evaluate the Higgs production cross sections and decay rates, normalized to the SM ones, as a function of the neutralino mass for the case of light neutralinos and supersymmetric parameters consistent with the EWBG conditions obtained in section 2. In section 5 we analyze possible Dark Matter candidates in our scenario. Finally we devote section 6 to our conclusions.

## 2 The light stop scenario and the electroweak phase transition

The realization of the EWBG scenario in the MSSM demands the lighter stop ($\tilde{t}$) to be mainly right-handed and with masses of the order of 100 GeV. Since in the MSSM the value of the SM-like Higgs mass is determined through radiative corrections by the stop masses ($m_{\tilde{t}}, m_Q$) and mixing parameter $X_t = A_t - \mu/\tan\beta$, such a light stop tends to



JHEP02(2013)001

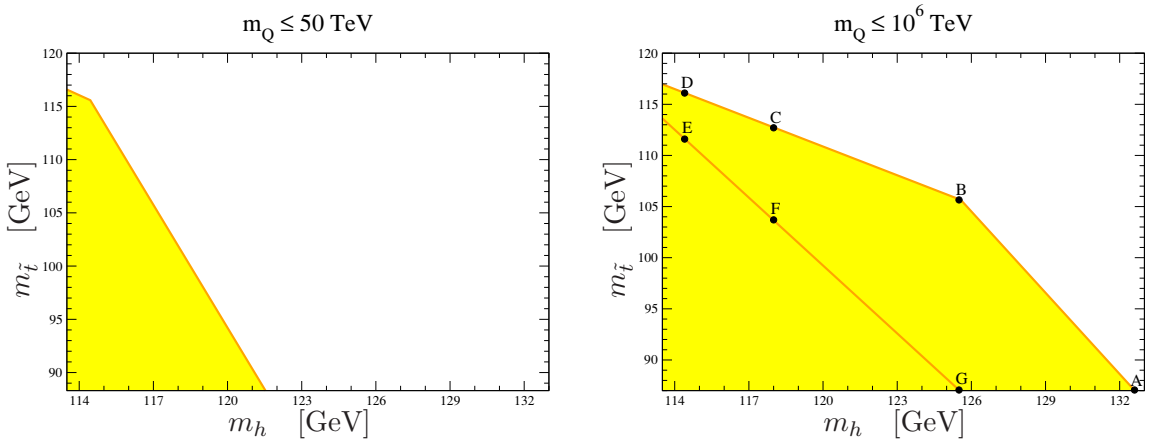


**Figure 1**. The window with $\langle\phi(T_n)\rangle/T_n \gtrsim 1$ for a gluino mass $M_3 = 700\,\text{GeV}$, $m_Q \leq 50\,\text{TeV}$ (left panel) and $m_Q \leq 10^6\,\text{TeV}$ (right panel).

| Point | A | B | C | D | E | F | G |
|---|---|---|---|---|---|---|---|
| $\lvert A_t/m_Q\rvert$ | 0.5 | 0 | 0 | 0 | 0.3 | 0.4 | 0.7 |
| $\tan\beta$ | 15 | 15 | 2.0 | 1.5 | 1.0 | 1.0 | 1.0 |

**Table 1**. Values of the fundamental parameters at the scale $m_Q = 10^6\,\text{TeV}$ corresponding to the benchmark points shown in the left panel of figure 1.

imply the presence of a light Higgs boson unless the heavy stop mass $m_Q$ is very large. In order to obtain Higgs boson masses above the LEP limit the heaviest stop mass must be much larger than 1 TeV. This implies that a simple one-loop analysis will not lead to reliable results since it will in general be affected by large logarithmic functions of ratios of the heavy stop scale to the weak scale. Such large logarithmic corrections may be efficiently resummed by means of a Renormalization Group (RG) improvement. In ref. [49] the technical framework for the treatment of the light stop scenario, in the presence of a very heavy stop, was defined by using an effective theory approach and it was subsequently applied to the EWBG scenario in ref. [41]. For completeness, and in order to define a few representative updated points, we present the results of such an analysis here.

In order to properly analyze the issue of EWBG we have complemented the zero temperature results with the two-loop finite temperature effective potential [28]. Light stops may be associated with the presence of additional minima in the stop-Higgs $V(\tilde{t}, h)$ potential, and therefore the question of vacuum stability is relevant and should be considered by a simultaneous analysis of the stop and Higgs scalar potentials. All points shown in figure 1 fulfill the vacuum stability requirement.[1]

For values of the heavy stop mass $m_Q$ below a few tens of TeV, the maximal Higgs mass that can be achieved consistent with a strong first order phase transition is about

[1]There is an apparent loss of perturbativity in the thermal corrections to the $\tilde{t}$ potential associated with the longitudinal modes of the gluon. In our work we considered that, due to their large temperature dependent masses, the terms proportional to the third power of their thermal masses in the high temperature expansion are efficiently screened and do not lead to any relevant contribution to the $\tilde{t}$ potential.



JHEP02(2013)001

122 GeV. The main reason is that larger values of the Higgs boson mass would demand large values of the mixing parameter $X_t$, for which the effective coupling $g_{hh\tilde{t}\tilde{t}}$ of the lightest stop to the Higgs is suppressed, turning the electroweak phase transition too weak. In the effective theory the coupling $g_{hh\tilde{t}\tilde{t}}$ is given by

$$g_{hh\tilde{t}\tilde{t}} \simeq h_t^2 \left(1 - \frac{X_t^2}{m_Q^2}\right)(1 + \Delta_g) \tag{2.1}$$

where $\Delta_g$ contains one-loop threshold and radiative corrections (see ref. [49] and figure 1 of ref. [51]). Such Higgs mass values, below 122 GeV, would not lead to an explanation of the Higgs signal observed at the LHC [42–48].

For larger values of the heaviest stop mass the logarithmic corrections to the Higgs mass increase and larger values of the Higgs mass may be obtained for the same value of $X_t/m_Q$, preserving the strength of the phase transition. In this paper we shall focus on benchmark points where $m_Q = 10^6$ TeV. This is represented in the right panel of figure 1, where it is shown that values of the Higgs mass as large as 132 GeV may be obtained for this value of $m_Q$ and (relatively large values of) $\tan\beta \simeq 15$, corresponding to point A. However any given point inside the EWBG region calculated at $m_Q = 10^6$ TeV and moderate $\tan\beta$ can also be conveniently obtained by decreasing $m_Q$ and increasing $\tan\beta$. Even for $\tan\beta \simeq 1$ values of the Higgs mass about 125 GeV may be obtained for $m_Q = 10^6$ TeV, as it is represented by point G in figure 1. The largest values of the Higgs mass are obtained for the largest possible values of the Higgs mixing parameter, which in turn leads to the smallest values of the lightest stop mass consistent with a strong electroweak phase transition. Points A and B have $\tan\beta \simeq 15$ while the rest of the points have smaller values of $\tan\beta$ as shown in table 1, which defines the values of the fundamental parameters for the benchmark points used in this work.[2] Finally let us stress that, although in this paper we concentrate on the MSSM case, the value of $m_Q$ can be considerably lowered in some non-minimal UV completions of the LSS [54].

## 3 Light neutralinos and the EWBG scenario

In this section, we shall study the effects of light neutralinos on the $Z$ and Higgs invisible width, as well as on the stop phenomenology within the EWBG scenario. As it was discussed in section 1, a light stop with relevant couplings to the Higgs (leading to a modification of the phase transition strength) has relevant implications for Higgs phenomenology: it induces an effective enhancement of about a factor two of the diphoton rate associated with Higgs production [50, 51]. Such an enhancement is not in conflict with data, but even larger enhancements of the $WW$ and $ZZ$ rates are induced, that seem to be in tension with the LHC data for $m_h \simeq 125$ GeV [52, 53]. The aim of this paper is to extend the analyses of refs. [52, 53] to the case of light neutralinos with masses below 60 GeV. This will open the Higgs (invisible) decay channel into neutralinos and then reduce the enhancement of the gauge boson rates, thereby alleviating the tension with LHC data. As it was already

[2] Notice that the parameters $A_t \simeq X_t$ as $\mu = \mathcal{O}(100\,\text{GeV}) \ll m_Q$ in the LSS.



JHEP02(2013)001

done in ref. [52] the study will be performed taking into account the correlation of the coupling $g_{hh\tilde{t}\tilde{t}}$ with the stop mass $m_{\tilde{t}}$ as well as the requirement of a strong first order phase transition. On the other hand, as in ref. [53], we will simplify the analysis by considering the values of Higgs interactions with higgsinos and gauginos to be supersymmetric-like and not the proper ones of the effective theory.[3]

### 3.1 Collider constraints on light stops

There have recently been many theoretical analyses on stop mass limits [55–61]. However as most of them do not fit the precise structure and freedom of the LSS we will consider in this section only experimental results.

Apart from their effect on Higgs physics, light neutralinos qualitatively modify the stop phenomenology, which also depends to a large extent on the mass of the lightest chargino. Charginos may be heavier or lighter than the lightest stop:

- If the lightest chargino is lighter than the stop, the latter is expected to decay in a two body decay channel $\chi_1^+ b$. The chargino will then subsequently decay into a $W$ (on-shell or off-shell) and the lightest neutralino or, in the presence of light third generation sleptons, into a $\tau$, a neutrino and the lightest neutralino. The first possibility is strongly constrained experimentally: a lower bound on the stop mass of about 150 GeV was obtained under the above assumptions [62–65].

- If the charginos are heavier than the lightest stop, then stops can decay through a two body decay channel,

$$\tilde{t} \to c\, \chi_1^0\,, \tag{3.1}$$

  or through a three (four) body decay channel provided that $m_{\tilde{t}} > m_W + m_b + m_{\chi_1^0}$ ($m_{\tilde{t}} < m_W + m_b + m_{\chi_1^0}$),

$$\tilde{t} \to b W^+ \chi_1^0 \quad (\tilde{t} \to_b \chi_1^0 \bar{f} f')\,, \tag{3.2}$$

  where the four-body channel appears through the exchange of a virtual $\chi_1^+$ or top quark. The three body decay is in general the dominant stop decay mode if kinematically allowed in this region of parameters. In addition, other decays may be present in the case of light sfermions, that may contribute to the decay amplitude in channels which do not involve the charged gauge bosons. An example, as mentioned above, would be a light $\tilde{\tau}$, or a light $\tilde{\nu}_\tau$ (both heavier than $\chi_1^0$ not to make the neutralino unstable), which may lead to final states including $\tau$ leptons and neutrinos, apart from a $b$-quark and a neutralino.[4] We have checked that for off-shell charginos and

[3] Supersymmetry implies equality of couplings of several interactions, which are modified when the heavy MSSM scalars are decoupled. Estimating the numerical value of each effective coupling is cumbersome [49] and since the couplings involved are weak couplings one expects the departures from their precise supersymmetric values to lead to subleading effects.

[4] In our analysis we impose $\tan\beta \leq 15$ from conservative EDM and baryon asymmetry density constraints [49]. For $\tan\beta \leq 15$ light staus do not essentially modify the Higgs phenomenology presented in this paper. However in the presence of cancellations in the EDMs chargino-neutralino contributions larger values of $\tan\beta$ ($\tan\beta \sim 60$) would be allowed and consequently light staus would enhance the diphoton Higgs decay rate [67, 68] as well as the baryon asymmetry production [69]. We leave this possibility for future studies.



JHEP02(2013)001

$m_{\tilde{t}} < m_W + m_b + m_{\chi_1^0}$, and values of $M_2$ and $\mu$ of order of the weak scale, the decays $\tilde{t} \to b\tau^+\tilde{\nu}_\tau$ or $\tilde{t} \to b\nu_\tau\tilde{\tau}^+$ become the dominant ones whenever one (or both) of these three body decay channels is kinematically allowed.

Searches at the LEP and Tevatron experiments have put very strong bounds on the lightest stop and neutralino masses using the two body decay channel (3.1). In fact by assuming $\mathrm{BR}(\tilde{t} \to c\ \chi_1^0) = 1$ LEP imposes $m_{\tilde{t}} \gtrsim 95\,\mathrm{GeV}$ and Tevatron requires $m_{\tilde{t}} - m_{\chi_1^0} \lesssim 35\,\mathrm{GeV}$ [66]. Therefore if there are no stop decay channels competing with the decay $\tilde{t} \to c\ \chi_1^0$ these experimental bounds imply $m_{\chi_1^0} \gtrsim 60\,\mathrm{GeV}$, which closes the Higgs decay into neutralinos. On the other hand when $\mathrm{BR}(\tilde{t} \to c\ \chi_1^0) < 1$, the stop mass lower bound becomes weaker. For that reason, and to realize the EWBG scenario ($87\,\mathrm{GeV} \lesssim m_{\tilde{t}} \lesssim 120\,\mathrm{GeV}$), additional light stop decay channels are required to permit sizable $\mathrm{BR}(h \to \chi_1^0\chi_1^0)$.[5]

Interestingly enough, assuming no tree-level flavor violating couplings the dominant loop-induced contributions to the two body decay channel, eq. (3.1), tend to be suppressed in the LSS discussed in this paper. Therefore, one can consider the possibility of a four body decay channel as the dominant one when neutralinos are heavy enough to kinematically forbid the three body decay channel. To quantify the previous statement, we will now consider the particular case of the LSS with a light right-handed stop $\tilde{t}$, small mixing in the stop sector $X_t \ll m_Q$, as preferred by the EWBG mechanism, and light charginos and neutralinos, while the rest of squarks and heavy Higgses are very heavy with a common mass $m_Q$. Considering only the contributions enhanced by large logarithmic factors depending on the ratio of the supersymmetry breaking scale to the weak scale, the partial width of the decay $\tilde{t} \to c\chi_1^0$ is given by [71–73]

$$\Gamma(\tilde{t} \to c\chi_1^0) = \frac{\alpha}{4} m_{\tilde{t}} \left(1 - \frac{m_{\chi_1^0}^2}{m_{\tilde{t}}^2}\right)^2 |f_L \epsilon|^2 \tag{3.3}$$

where

$$f_L = \sqrt{2}\left[\frac{2}{3}(c_W N_{11} + s_W N_{12}) + \left(\frac{1}{2} - \frac{2}{3}s_W^2\right)\left(\frac{N_{12}}{s_w} - \frac{N_{11}}{c_w}\right)\right] \tag{3.4}$$

with $N_{11}$ ($N_{12}$) the Bino (Wino) component of the lightest neutralino, respectively, and

$$\epsilon = \frac{\alpha}{4\pi s_W^2} \frac{V_{tb}^* V_{cb} m_b^2}{2m_W^2 \cos^2\beta} \left[\frac{m_t A_b}{m_Q^2} - \left(3 + \frac{A_b^2}{m_Q^2}\right)\frac{m_t X_t}{m_Q^2}\right] \log\frac{\Lambda_S^2}{m_W^2} \tag{3.5}$$

is a radiatively induced mixing between the light stop and the left-handed charm squark, with $\Lambda_S$ the messenger scale where supersymmetry is transmitted to the observable sector. Notice that consistently with the assumption of small mixing in the stop sector we have expanded in eq. (3.5) the mixing angle to first order in the expansion parameter $m_t A_{t,b}/m_Q^2$. Even for sizable values of the mixing parameters in the sbottom and/or stop sectors, $A_t, A_b \simeq \mathcal{O}(m_Q)$, the mixing $\epsilon$ has the extra suppression $m_t/m_Q$, and hence the

[5] See for instance ref. [70] for constraints on light stops and neutralinos in some scenarios where different channels compete.



JHEP02(2013)001

partial width $\Gamma(\tilde{t} \to c\chi_1^0)$ is very suppressed at the considered order. The remaining loop contributions are not enhanced by large logarithmic factors and therefore in the LSS the four body decay channel can efficiently compete with the two body decay channel and can become the dominant one when the three body decay channel is kinematically forbidden.

The three and four body decay final states, eq. (3.2), are similar to those with light charginos previously discussed, but now the decays proceed through the off-shell chargino production. It would therefore be interesting to extend the analysis of ref. [63] to the case where the chargino generated by the stop decay are not on-shell. The presence of light third generation sleptons can affect the final state of the stop decay and a careful analysis of the experimental constraints must be performed considering the stop decay channel $\tilde{t} \to b\tau^+\nu_\tau\chi_1^0$. Moreover constraining the stop mass would require different strategies if the lightest neutralino were unstable, as in the presence of $R$-parity violation.

Light stops and light neutralinos can also affect the top quark phenomenology, since the decay channel

$$t \to \tilde{t}\chi_1^0 \tag{3.6}$$

opens up. This decay channel leads to the decay width [74]

$$\Gamma(t \to \tilde{t}\chi_1^0) \simeq \frac{1}{16\pi}\left(\frac{2e}{3c_W}\right)^2 m_t \left(1 - \frac{m_{\tilde{t}}^2}{m_t^2}\right)^2 \tag{3.7}$$

where for simplicity we have omitted the neutralino mass. In this way the decay width for the channel $t \to \tilde{t}\chi_1^0$ is smaller than about 150 MeV for $m_{\tilde{t}}$ in the range 90-115 GeV which is significantly smaller than the experimental error on the top width $\Gamma_t = 2.0^{+0.47}_{-0.43}$ GeV [75].

### 3.2 Higgs and Z invisible widths

As mentioned above, we are interested in studying the effect of light neutralinos on the Higgs production rates in the EWBG scenario. These effects are induced by a modification of the Higgs decay width. For $2m_{\chi_1^0} < m_h$, the Higgs decay channel into a pair of lightest neutralinos $\chi_1^0\chi_1^0$ is open with a tree-level width

$$\Gamma(h \to \chi_1^0\chi_1^0) = \frac{G_F m_W^2}{2\sqrt{2}\pi} m_h \left(1 - \frac{4m_{\chi_1^0}^2}{m_h^2}\right)^{3/2} g_{h11}^2 \,, \tag{3.8}$$

where the coupling of the Higgs to the lightest neutralino, $g_{h11}$, depends on the product of the gaugino and Higgsino components of the lightest neutralino. For large values of the pseudo-scalar mass $m_A$ (i.e. $\alpha \simeq \beta - \pi/2$), the coupling $g_{h11}$ is given by

$$g_{h11} = (N_{12} - \tan\theta_W N_{11})(\sin\beta N_{1u} - \cos\beta N_{1d}) \,, \tag{3.9}$$

where $N_{1u}$ and $N_{1d}$ are the neutralino components along the Higgsino that couples to up and down right-handed quarks, and $N_{11}$ and $N_{12}$ denote the Bino and Wino components, respectively. Due to the LEP chargino mass constraints, a lightest neutralino with mass below 60 GeV must be predominantly Bino. Hence, the Higgs decay rate depends on the Higgsino component and gets larger for smaller values of $\mu$.



JHEP02(2013)001

On the other hand the relevant Higgsino component, and thus the decay width $\Gamma(h \to \chi_1^0\chi_1^0)$, becomes more important for small values of $\tan\beta$, for which the coupling of the lightest neutralino to the $Z$ boson

$$g_{Z11} = \frac{1}{2}\left(|N_{1u}|^2 - |N_{1d}|^2\right) \tag{3.10}$$

and thus the invisible $Z$ decay width

$$\begin{aligned}\Gamma(Z \to \chi_1^0\chi_1^0) &= \frac{G_F}{\sqrt{2}\,6\pi} m_Z^3 \left(1 - \frac{4m_{\chi_1^0}^2}{m_Z^2}\right)^{3/2} g_{Z11}^2 \\ &\simeq 0.332\ \text{GeV}\ g_{Z11}^2 \left(1 - \frac{4m_{\chi_1^0}^2}{m_Z^2}\right)^{3/2} ,\end{aligned} \tag{3.11}$$

get suppressed.[6]

Therefore, depending on $\tan\beta$, $\mu$ and $M_2$, the composition of the lightest neutralino is constrained by the LEP invisible $Z$ width measurement $\Gamma_{inv} = 499.0 \pm 1.5\,\text{MeV}$ [76], which translates into the 95% CL upper bound

$$\Gamma(Z \to \chi_1^0\chi_1^0) \lesssim 0.5\ \text{MeV}\ . \tag{3.12}$$

The subsequent lower bound on $\mu$ is shown in figure 2 for $M_2 = 200\,\text{GeV}$ and various values of $\tan\beta$ (left panel) and $M_1$ (right panel). The solid curves correspond to the constraint (3.12) while the dashed lines correspond to the LEP chargino mass bound $m_{\chi_1^\pm} > 94\,\text{GeV}$ [76]. The region below each line in figure 2 is excluded at the 95% CL.. As can be seen from figure 2, for small values of $\tan\beta$ the strongest bounds on $\mu$ come from direct searches on charginos, while for large values of $\tan\beta$ the constraints mainly come from the invisible width measurement. Notice that for $M_2 = 200\,\text{GeV}$, values of $\mu \simeq 200\,\text{GeV}$ are well within the allowed region independently of the value of $\tan\beta$. The results in figure 2 are consistent with general analyses performed in the context of the MSSM [77].

On the other hand one can obtain constraints on the invisible Higgs decay (3.8) by looking at signatures of jets plus missing energy. After using $1\,\text{fb}^{-1}$ of data the analysis of this signature by the ATLAS experiment [78] shows that the Higgs production times the invisible decay branching ratio must be less than four times the SM Higgs production [79, 80] which puts no constraint in our model. However extrapolating these results to $5\,\text{fb}^{-1}$ of data for $m_h \simeq 125\,\text{GeV}$ sets a more stringent constraint on models with dominant gluon fusion production [81] which, for the LSS, would approximately correspond to

$$\frac{\sigma(gg \to h)}{\sigma(gg \to h)_{SM}} \times \text{BR}(h \to \text{inv}) \lesssim 1.9 \quad \text{at 95\% C.L.} \quad (m_h \simeq 125\,\text{GeV})\ . \tag{3.13}$$

In practice this bound would require cross section times the dominant invisible decay branching ratio enhancement to be smaller than 2. In most of the cases analyzed in this article the cross section enhancement is slightly about a factor 2 and the branching ratio not larger than 0.85 and hence this constraint tends to be fulfilled (although there are some residual regions in the parameter space which are not compatible with it). On the other hand this bound allows regions that can be already excluded because of other

[6] Indeed it vanishes for $\tan\beta = 1$.



JHEP02(2013)001

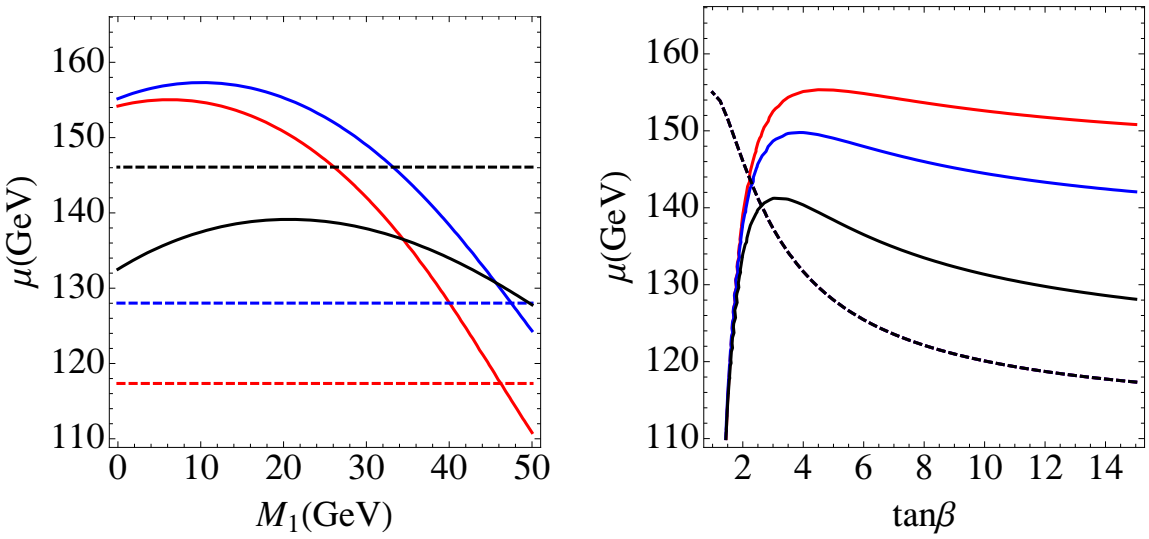


**Figure 2**. Left panel: allowed region in the $(M_1, \mu)$-plane, for $M_2 = 200$ GeV, from the constraint in eq. (3.12) for $\tan\beta = 15$ [above the intermediate (red) solid line], 5 [above the upper (blue) solid line] and 2 [above the lower (black) solid line]. For comparison we also show the corresponding allowed regions (above the corresponding dashed lines) for $\tan\beta = 15$ (lower line) to $\tan\beta = 2$ (upper line) from bounds on the lightest chargino mass $m_{\chi_1^\pm} > 94\,\text{GeV}$. Right panel: the same in the $(\mu, \tan\beta)$-plane for $M_1$ =20 GeV [upper (red) solid], 30 GeV [intermediate (blue) solid] and 40 GeV [lower (black) solid].

observables. In particular in the LSS values of $\text{BR}(h \to \text{inv}) \gtrsim 0.7$ lead to Higgs decay rates into SM particles that are in general significantly smaller than the experimental ones (see figures 3–6).[7] We shall further comment on this in the next section.

As a final remark, we stress that the above constraints hold also for unstable neutralinos provided their lifetime is much larger than the size of the detector. This situation can arise, for example, in the presence of R-parity violation. For instance, if the R-parity violation affects only the squarks, the stop can gain an extra two-body decay channel with a width that, depending on the coupling strength, may be comparable or larger than the one of the usual stop decay modes, and therefore the bounds discussed in section 2 would have to be revised. The neutralino, instead, can have a five-body decay via off-shell top and stops, and an off-shell W from the top. The additional number of particles in the decay, together with hypercharge and weak couplings, leads to a $\mathcal{O}(10^6)$ suppression of the neutralino width compared with the stop one. The R-parity violation can thus modify the stop phenomenology with neutralinos that may remain stable at collider scales, and hence the products of the Higgs decay into neutralinos will remain invisible.[8]

[7] This observation mirrors the result of the ATLAS analysis fitting multiple decay channels and leading to $\text{BR}(h \to \text{inv}) \lesssim 0.84$ at 95% C.L. [82] after profiling on gluon fusion and diphoton enhancement factors. Indeed for any model predicting particular values of the gluon and diphoton enhancement factors we expect a stronger bound on $\text{BR}(h \to \text{inv})$ than the ATLAS one. In particular for the LSS model analyzed in this paper we have checked that there is an approximate upper bound on $\text{BR}(h \to \text{inv}) \lesssim 0.7$ as we have mentioned.

[8] Even if both stop and neutralino would decay promptly, a five body decay of a light neutralino necessarily implies soft decay products. These would therefore not appear in standard Higgs searches and these decay channels will thus practically remain "invisible".



JHEP02(2013)001

## 4 LHC Higgs signatures correlation and dependence on $m_{\chi_1^0}$

As previously discussed, in the EWBG scenario, light stops with relevant couplings to the Higgs induce modifications to the rates of gluon fusion Higgs production and Higgs decay into gluon and photon pairs, which tend to be significant. In particular deviations from the SM production and decay rates yield some tension with LHC data [42–47] for $m_h \simeq 125\,\text{GeV}$ [52, 53]. In comparison with ref. [53] our results present smaller deviations of the gluon fusion Higgs production rates from the SM values. This is due to the fact that we consider the proper correlation between the Higgs-stop effective coupling $g_{hh\tilde{t}\tilde{t}}$ and the stop mass $m_{\tilde{t}}$ through the mixing $A_t$, and that we do not neglect the stop mixing effects in the loop-induced production and decay rates. As an example of the relevance of such effects, the lightest stops in the EWBG scenario are obtained through relatively large $X_t/m_Q$. In such a case, the large enhancement of the gluon production rate obtained by small $m_{\tilde{t}}$ is partially suppressed by the reduction of $g_{hh\tilde{t}\tilde{t}}$ in eq. (2.1).

In this section we shall re-analyze the LSS Higgs phenomenology studied in refs. [52, 53] and determine how the Higgs signatures are affected by the additional presence of a light neutralino. In order to study the light neutralino effects we consider values of the supersymmetric parameters that are consistent with the bounds on the $Z$ invisible width (3.12), as shown in figure 2. Results for several benchmark points exhibited in figure 1 are presented in figures 3–6. On the right panels of these figures we present the dependence on the neutralino mass $m_{\chi_1^0}$ of the relevant Higgs decay branching ratios, while in the left panels we present the ratios of the gluon fusion and weak boson fusion production cross sections times the branching rates for SM channels with respect to their corresponding values in the SM. In the right panels we also plot the next-to-lighest neutralino and lighest chargino masses, $m_{\chi_2^0}$ and $m_{\chi_1^+}$. We consider large values of $m_A$ for which the tree-level coupling of the Higgs to the SM fields is the same as in the SM. Therefore, the ratio of weak boson fusion production times tree level Higgs decay rates to SM ones is simply given by the quotient of the branching ratios. Instead the ratios of gluon fusion production induced processes are strongly modified by the presence of light stops. A few general comments are here in order.

- The considered cases in this section have charginos always off-shell in the decay chain $\tilde{t} \to b\chi_1^+ \to bW^+\chi_1^0$, or similarly $\tilde{t} \to b\tilde{\tau}^+\nu_\tau$ ($\tilde{t} \to b\tilde{\nu}_\tau\tau^+$) in the presence of a light stau (tau sneutrino).

- For $M_2 = 200$ GeV, values of $\mu \gtrsim 180\,\text{GeV}$ lead to consistency with all experimental constraints and to chargino masses such that the two body decay of the stop into an on-shell chargino and a bottom quark is forbidden in the whole parameter space under study.

- The effect of the neutralino on Higgs physics is much stronger for small $\tan\beta$ due to an increase in the Higgsino component of the lightest neutralino. On the other hand for the same mass parameters, $m_{\chi_1^\pm}$ and $m_{\chi_2^0}$ tend to decrease in value.

Figure 3 shows the masses $m_{\chi_1^+}$ and $m_{\chi_2^0}$, the Higgs production rates normalized to the SM ones and the Higgs decay branching ratios at point $B$, with $\tan\beta = 15$, as a function



JHEP02(2013)001

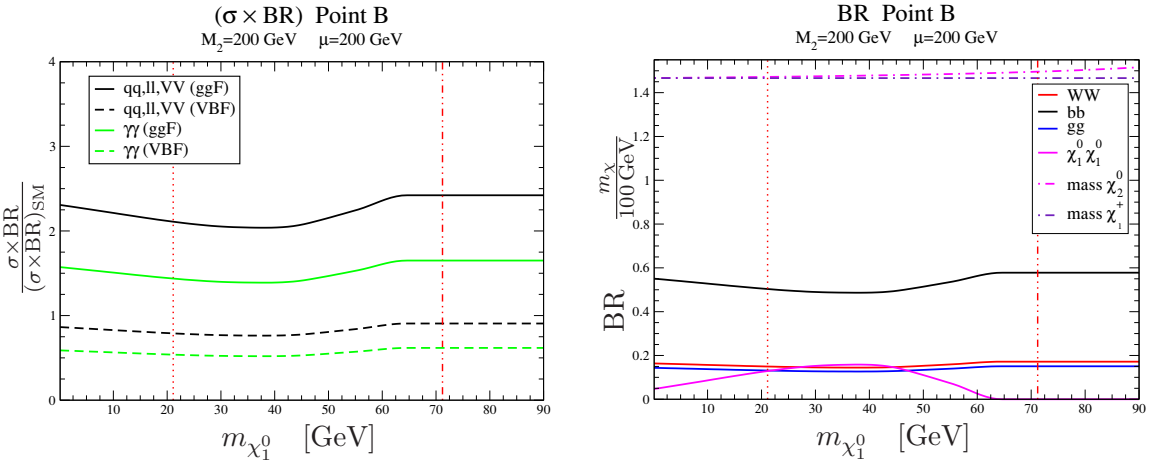


**Figure 3**. $(\sigma\times\mathrm{BR})/(\sigma\times\mathrm{BR})_{\mathrm{SM}}$ of the Higgs (left panel) and BR of the Higgs (right panel, channels with BR$<0.1$ are omitted) as a function of $m_{\chi_1^0}$ at point B of figure 1 for $M_2 = \mu = 200\,\mathrm{GeV}$. The Higgs mass is about 125 GeV. The lightest chargino and next-to-lightest neutralino (lower and upper dot-dashed lines in the right panel) are heavier than the light stop. The vertical dot-dot-dashed line corresponds to the Tevatron lower bound on the lightest neutralino assuming $\mathrm{BR}(\tilde{t}\to c\,\chi_1^0) = 1$. On the left (right) of the vertical dotted line the stop can decay as in eq. (3.2) with a real (virtual) W boson.

of the neutralino mass. We have chosen $\mu = 200\,\mathrm{GeV}$, which widely overcomes the lower bound on this parameter from the invisible $Z$-width for this value of $\tan\beta$. For $m_{\chi_1^0}$ smaller (larger) than 20 GeV the three body decay (3.2) is allowed (forbidden). The Higgs mass is about 125.5 GeV, consistent with the LHC observation.

For $m_h \simeq 125.5\,\mathrm{GeV}$, both the LHC and Tevatron data are overall compatible with SM Higgs rates within statistical errors. However, both ATLAS and CMS see an enhancement in the diphoton channel [42–47], with the best fit to the diphoton production cross section being $(1.90 \pm 0.50)$ and $(1.56 \pm 0.43)$ times the SM one, for a Higgs mass 126.5 GeV and 125 GeV, respectively. CMS and ATLAS also report results discriminating between the vector boson fusion and gluon fusion production channels. CMS shows enhancements of order 2 times and 1.5 times the SM cross section in the weak boson fusion and gluon fusion production channels, respectively, but the errors are large and both channels are only about $1\sigma$ above the SM predictions. Similar results are obtained at ATLAS, which shows central values of order 2 times the SM cross sections in both production channels. In the $ZZ$ channel, ATLAS and CMS are in good agreement with SM predictions [42–47], but with rates about $(1.3 \pm 0.6)$ and $\left(0.7^{+0.5}_{-0.4}\right)$ times the SM one, and hence also consistent with slight suppressions or enhancements of these rates. Similarly, the best fit to the ATLAS and CMS $WW$ production rates [42–48] are about $(1.4 \pm 0.5)$ and $(0.6^{+0.5}_{-0.4})$ times the SM one, respectively. CMS also shows a large suppression of $WW$ production in the vector boson fusion channel, but with a very large error. CMS also reports a suppression of $\tau\tau$ production in the vector boson fusion channel [43, 47]. No such suppression is seen in the gluon fusion channel. Overall, considering all the production and decay channels explored at the LHC, the best fit performed at CMS shows a suppression of the vector boson fusion



JHEP02(2013)001

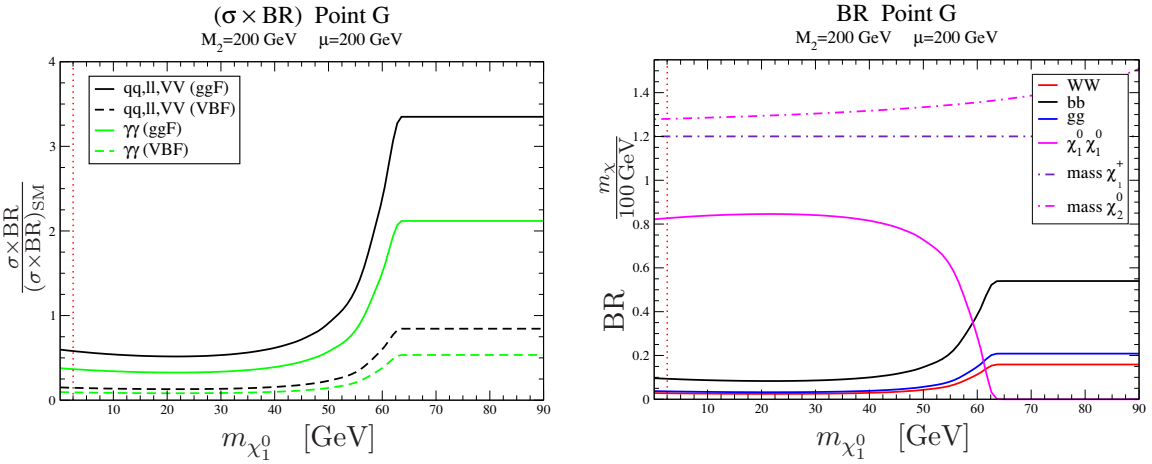


**Figure 4**. The same as figure 3 but for point G and $M_2 = \mu = 200\,\text{GeV}$. The Higgs mass is about 125 GeV.

induced rates with respect to those expected in the SM and gluon fusion induced rates that are consistent with the SM ones. As we will show, such overall behavior is consistent with the predictions of the LSS in the presence of light neutralinos.

As it is highlighted in figure 3, for $m_{\chi_1^0} \gtrsim 63\,\text{GeV}$ the Higgs cannot decay into neutralinos. In such a case the Higgs production via gluon fusion is enhanced by a factor larger than two. Then the subsequent Higgs decay into weak bosons, whose rate is unmodified by light stops at leading order, is enhanced by the same factor of two. This enhancement factor is instead suppressed by $\sim 25\%$ if the Higgs decays into photons because of the stop destructive-interference contribution. If $m_{\chi_1^0} \lesssim 63\,\text{GeV}$ the Higgs invisible width increases. However for relatively large values of $\tan\beta$, as point B, and for $\mu = M_2 = 200\,\text{GeV}$, the coupling $g_{h11}$ is suppressed, and opening kinematically the Higgs decay channel into neutralinos reduces the visible branching ratios by at most 10%. In conclusion, for point B we confirm the result of the previous analyses [52, 53]: for heavy neutralinos there is tension with data, independently of the specific choice of $\mu$ and $M_2$. Moreover, for smaller values of the neutralino mass the tension persists, unless one assumes smaller values of $\mu$ and/or $M_2$ than those considered here, $\mu = M_2 = 200\,\text{GeV}$ (see comments on figure 8 for more details).

In order to see at work the mechanism of invisible Higgs decay into neutralinos for $\mu \approx M_2 \approx 200\,\text{GeV}$, we have to consider small values of $\tan\beta$ for which the coupling $g_{h11}$ is sizable. In particular this is the case for point G in figure 1. Figure 4 shows the corresponding results for point G, for which $\tan\beta$ is close to 1 and the Higgs boson mass is still about 125 GeV.[9] In this case the Higgsino $\tilde{H}_u$ component of the lightest neutralino increases and hence the decay width of the Higgs into the lightest neutralino can be more significant even for $\mu = M_2 = 200\,\text{GeV}$. Indeed in the region in which the Higgs is allowed to decay into neutralinos its branching ratio tends to be the dominant one. On the other hand in the large $m_{\chi_1^0}$ region one obtains enhancement factors in the Higgs production rates

[9] With respect to point B the smaller tree-level Higgs mass due to the decrease of $\tan\beta$ is compensated by rising the mixing parameter $X_t$ in the radiative contributions.



JHEP02(2013)001

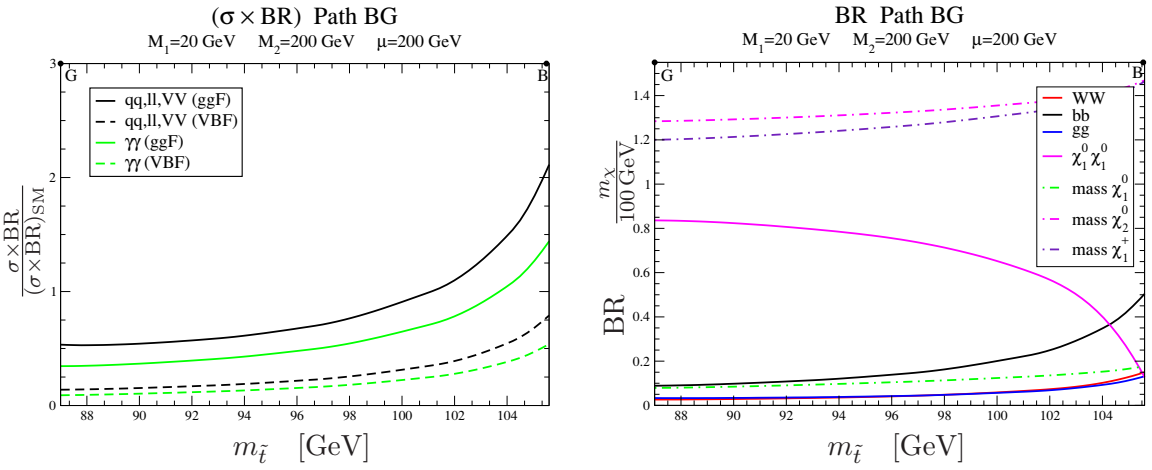


**Figure 5**. Evolution along the path BG of figure 1 of $\sigma \times \mathrm{BR}/(\sigma \times \mathrm{BR})_{SM}$ (left panels) and BR (right panels) for $M_2 = \mu = 200\,\mathrm{GeV}$ and $M_1 = 20\,\mathrm{GeV}$.

mediated via gluon fusion which are even larger than for point B. These large enhancement factors are, however, compensated by the large increase of the Higgs invisible width for small values of the neutralino mass. Values of the vector-boson production rate about 60% (or less) the SM value are obtained in the gluon fusion induced channels for small neutralino mass. The weak boson fusion production signatures are strongly suppressed with respect to the SM case. Such values are in tension with present data as the predicted diphoton rate is small compared to the current results at this invariant diphoton mass in both the gluon fusion channel as well as in the channel with two jets, in which vector boson fusion production contributes in a significant way. Moreover, the rate of invisible Higgs production is large, being in tension with the current bounds on this rate, eq. (3.13). In conclusion, at point G, for heavy neutralinos the enhancement of signatures induced through gluon fusion is in tension with data, as already observed in the literature. The suppression mechanism via light neutralinos leads to both gluon fusion and vector boson fusion induced rates that are too small, and also in tension with data. Values of the neutralino mass in the range 55-57 GeV lead to the best description of data, and require extra stop decay channels beyond the $c\chi^0$ and $W^+b\chi^0$ ones to be consistent with stop physics. The predicted rates of the signatures induced through vector boson fusion are about half of the SM values. In order to compare with data, however, a better understanding of the dijet channel rates coming from the gluon fusion Higgs production, whose rate in the LSS is significantly larger than in the SM, must be achieved.

As we have seen from figures 3 and 4 the dilution effect of the Higgs invisible decay, that is mainly governed by $\tan\beta$ (when the channel is kinematically accesible), vanishes for point B ($\tan\beta = 15$) and it is maximized for point G ($\tan\beta \simeq 1$). Both points are hence in tension with data for very light neutralinos. Along the path BG this effect varies continuously and one can find all intermediate cases. We illustrate the variation of this effect in figure 5 which shows the Higgs production rates with respect to the SM values (left panel) and the Higgs branching ratios (right panel) as a function of the stop mass along



JHEP02(2013)001

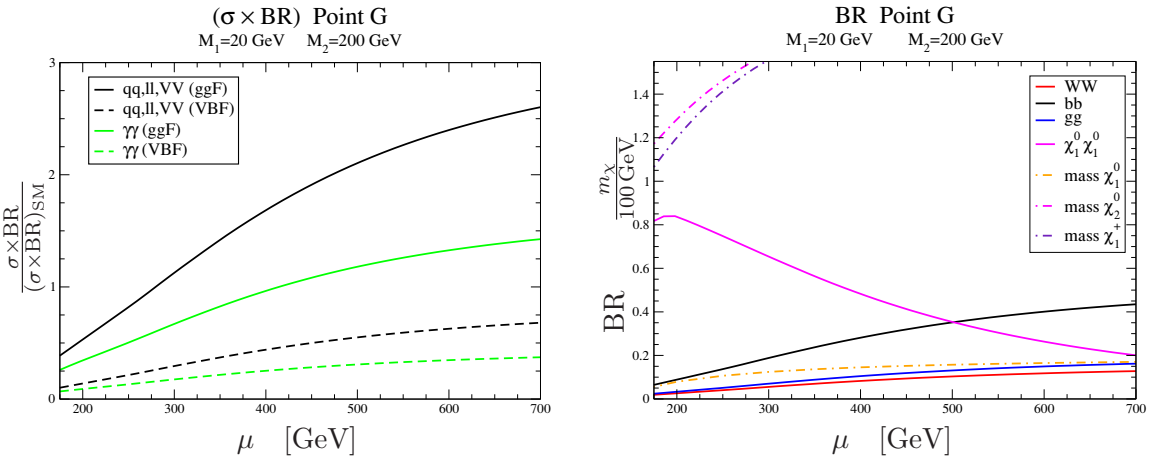


**Figure 6**. $(\sigma\times\mathrm{BR})/(\sigma\times\mathrm{BR})_{\mathrm{SM}}$ of the Higgs (left panel) and BR of the Higgs (right panel, channels with BR$<0.1$ are omitted) as a function of $\mu$ at point G of figure 1 for $M_1 = 20\,\mathrm{GeV}$ and $M_2 = 200\,\mathrm{GeV}$. The Higgs mass is about 125 GeV. The lightest chargino [dot-dashed (indigo) line in the right panel] is heavier than the stop.

the path BG.[10] In figure 5, where $m_{\chi_1^0} \approx 15\,\mathrm{GeV}$, better compatibility with LHC data is reached at larger stop masses ($m_{\tilde{t}} \approx 104\,\mathrm{GeV}$ with $\tan\beta \simeq 5$). No significant variation of these results would be obtained for $m_{\chi_1^0} \simeq 40\,\mathrm{GeV}$, for which the three body $W^+ b\chi_1^0$ decay channel would be kinematically forbidden.

For smaller stop masses (larger stop mixing) along the path BG, $\tan\beta$ decreases and the Higgs branching ratios to the visible sector are excessively reduced because of the large invisible decay width. Nevertheless, this does not exclude the EWBG region at small stop mass values. Better agreement with data at smaller stop masses can be achieved by reducing $\mathrm{BR}(h \to \chi_1^0\chi_1^0)$ in several ways: **i)** By assuming larger $m_{\chi_1^0}$; **ii)** By reducing $m_Q$, which allows to increase $\tan\beta$ for a given $m_{\tilde{t}}$; and, **iii)** By considering larger $\mu$ and to a lesser extent $M_2$, as it is illustrated in figure 6 for point G. We can see that, for the values of $M_1$ and $M_2$ considered in figure 6, better agreement with experimental data can be achieved for values of $\mu$ in the range $300\,\mathrm{GeV} \lesssim \mu \lesssim 400\,\mathrm{GeV}$. The ratio of the $h \to ZZ$ rate to the $h \to \gamma\gamma$ rate becomes larger for larger values of $\mu$, due to a suppression of the chargino effects, which tends to compensate the negative contributions to the $h \to \gamma\gamma$ amplitude induced by the light stops.

In general, we see that once the light neutralino effects are considered, consistency of the $gg \to h \to ZZ, WW, \gamma\gamma$ results with experimental data [42–47] may be restored. Higgs invisible decay branching ratios of order 30 – 60 % lead to the best description of current LHC Higgs results. These invisible width contributions may be obtained by adjusting the value of $\mu$, and hence the Higgsino component, in the case of very light neutralinos, or by taking values of the neutralino mass close to $m_h/2$, for low values of $\mu$. For fixed $\mu$ and $m_{\chi_1^0}$, one can also adjust $\tan\beta$ by varying $m_Q$ and hence obtain the desirable invisible width for $m_h \simeq 125.5\,\mathrm{GeV}$. All vector boson fusion induced channels tend to be suppressed due to

[10] Many paths in the full parameter space have the same projection in the plane $(m_h, m_{\tilde{t}})$ and fulfill the condition $v(T_n)/T_n \gtrsim 1$. The path we have considered is that with $v(T_n)/T_n \simeq 1$.



JHEP02(2013)001

the increase of the Higgs width, and this is consistent with the overall behavior observed at the CMS experiment. However, the experimental value of the rate of the dijet $h \to \gamma\gamma$ channel at the ATLAS and CMS experiments is currently larger than the SM one at the $1\sigma$ level. The main contribution to this channel at ATLAS and CMS is expected to come from vector boson fusion production. Therefore, the vector boson fusion channel $h \to \gamma\gamma$ imposes the strongest constraint on the realization of the LSS with light neutralinos within current experimental data. However, as stressed above, the contribution to the dijet channel from gluon fusion production may be larger in the LSS than in the SM, and therefore imparing a naive comparison of the vector boson fusion predictions with the dijet channel data.

## 5 Dark matter

A relevant question regarding the lightest neutralino we are considering is whether it can be a thermal WIMP. The low values of its mass determine that the neutralino co-annihilation with stops and charginos becomes subdominant, as well as the s-channel annihilation via Higgs bosons. The only relevant channel then is the one mediated by a $Z$ gauge boson. However constraints on the invisible $Z$ width determine that this channel might not always be efficient enough to accomodate the cosmological thermal DM abundance of the Universe.

An example that is compatible with the observed DM arises when, for instance, $m_{\chi_1^0} = 35 - 40\,\text{GeV}$ for $g_{Z11} \simeq 0.05$ [83].[11] These two conditions can be easily reproduced in the LSS, as it is shown in figure 7. In the left panel of figure 7 we plot the contour line $g_{Z11} = 0.05$ in the $(\mu, \tan\beta)$-plane for $M_2 = 200\,\text{GeV}$ and $M_1 = 55\,\text{GeV}$. Taking the constraint $m_{\chi_1^+} \gtrsim 95\,\text{GeV}$ [76], we exclude the region on the left of the thick dashed (red) curve. As the plot shows this constraint is stronger than condition (3.12) [excluding the region on the left of the thin dashed (blue) curve] for the considered parameter choice. Notice that the contour lines $m_{\chi_1^0} = 35\,\text{GeV}$ [thin dotted (red) curve], $m_{\chi_1^+} = 95\,\text{GeV}$ and $g_{Z11} = 0.05$ cross at the same point, which means that for $M_2 = 200\,\text{GeV}$ the parameter $M_1$ needs to be smaller than 55 GeV in order to fulfill the above conditions on $g_{Z11}$, $m_{\chi_1^+}$ and $\Gamma(Z \to \chi_1^0\chi_1^0)$. On the other hand by assuming $\tan\beta \lesssim 15$ as imposed by EWBG [41] one finds that the conditions $M_2 = 200\,\text{GeV}$, $m_{\chi_1^0} = 35$ and $g_{Z11} \simeq 0.05$ cannot be fulfilled with $M_1$ smaller than 40.6 GeV (case plotted in the right panel of figure 7). Moreover for such a value of $M_1$ the constraints on $\Gamma(Z \to \chi_1^0\chi_1^0)$ and $m_{\chi_1^+}$ are satisfied.

Summarizing once one fixes $M_2 = 200\,\text{GeV}$, for $40.6\,\text{GeV} \leq M_1 \leq 55\,\text{GeV}$ and $2.4 \leq \tan\beta \leq 15$, it is possible to properly choose $\mu$ in order to obtain the correct DM density and satisfy all experimental as well as EWBG constraints. Since the points in figure 1 are roughly independent of $M_1$, $M_2$ and $\mu$, the interval in $\tan\beta$ parametrizes univocally the BG path if one imposes $m_h = 125.5\,\text{GeV}$ (as well as $m_Q = 10^6\,\text{TeV}$ and $v(T_n) \simeq T_n$). Using this parametrization we plot the production cross-sections and Higgs branching ratios along the BG path in figure 8. As compared with figure 5 the production cross-sections are smaller even though in the latter the neutralino is lighter than 35 GeV. This is due to the smaller

[11] Notice that we can consistently produce the observed thermal DM density for larger (smaller) values of $m_{\chi_1^0}$ if $g_{Z11} \lesssim 0.05$ ($g_{Z11} \gtrsim 0.05$) provided that condition (3.12) is satisfied.



JHEP02(2013)001

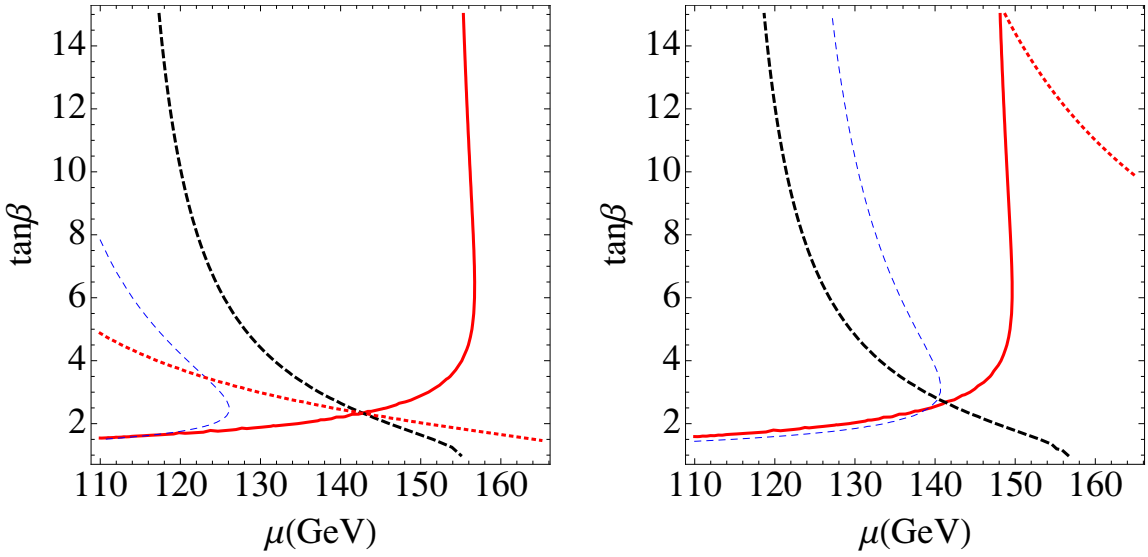


**Figure 7**. Left panel: contour plots of $g_{Z11} = 0.05$ [thick solid (red)] for $M_2 = 200\,\text{GeV}$ and $M_1 = 55\,\text{GeV}$, $m_{\chi_1^+} = 95\,\text{GeV}$ [thick dashed (black): allowed region on its right], $m_{\chi_1^0} = 35\,\text{GeV}$ [thin dotted (red)] and $\Gamma(Z \to \chi_1^0\chi_1^0)$=0.5 MeV [thin dashed (blue): allowed region on its right]. Right panel: the same as in the left panel but with $M_1 = 40.6\,\text{GeV}$.

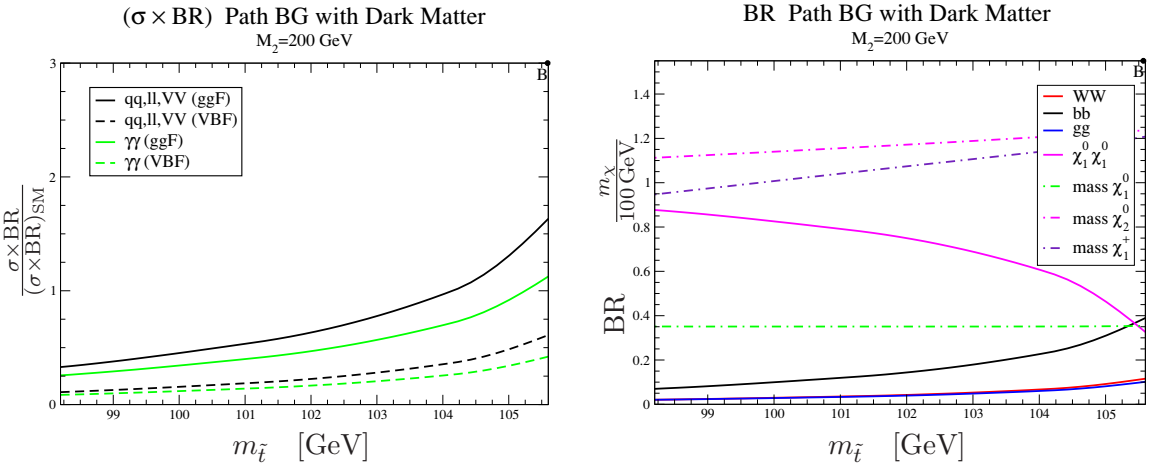


**Figure 8**. Evolution along the path BG of figure 1 of $\sigma \times \text{BR}/(\sigma \times \text{BR})_{SM}$ (left panels) and BR (right panels) for $M_2 = 200\,\text{GeV}$. $M_1$ and $\mu$ are fixed such that $m_{\chi_1^0} = 35\,\text{GeV}$ and $g_{Z11} = 0.05$.

values of $\mu$ that are used to achieve $g_{Z11} = 0.05$.[12] The best agreement with LHC data corresponds to values of the stop mass $m_{\tilde{t}} \simeq 105\,\text{GeV}$.

For neutralino masses larger than 35-40 GeV (but still smaller than $m_Z/2$), and/or $g_{Z11} > 0.05$ the neutralinos would yield too small thermal relic density today and they could just be a component of DM in the Universe. On the other hand, for masses lighter

[12]Indeed, as stressed in section 4 the production cross-sections rates presented in previous sections can all be increased or decreased by moving $\mu$ and $M_2$ away from the considered values, $\mu = 200\,\text{GeV}$ and $M_2 = 200\,\text{GeV}$.



JHEP02(2013)001

than 35-40 GeV and/or $g_{Z11} < 0.05$, if the lightest neutralinos were the LSP they would overclose the Universe. There should exist therefore a lighter supersymmetric particle into which the neutralino could decay. The possible candidates would be either light gravitinos or axinos.

A light enough gravitino leading to neutralino decays at times previous to the nucleosynthesis era would be an obvious choice that would lead to no cosmological constraints. Moreover one could demand this lifetime to be large enough not to affect the collider constraints. The reheating temperature should be small enough to avoid overproduction of gravitinos in the early Universe, but larger than $\mathcal{O}(100\,\text{GeV})$ in order to allow the mechanism of EWBG.

For small values of the gravitino mass the thermal gravitino relic density is given by [84]

$$\Omega_{3/2}h^2 \simeq 0.5 \left(\frac{M_{\tilde{g}}}{1\text{ TeV}}\right)^2 \frac{100\text{ MeV}}{m_{3/2}} \frac{T_R}{10^6\text{ GeV}}\,, \tag{5.1}$$

where $M_{\tilde{g}}$ is the gluino mass and $T_R$ the reheating temperature. Therefore for gravitino masses of order of a few tens of MeV, reheating temperatures smaller than about $10^5$ GeV are necessary in order to recover agreement with the observed DM density. On the other hand, for a bino-like neutralino, the neutralino width decaying into a photon and a gravitino is given by

$$\tau_{\chi_1^0} \simeq 8 \times 10^7\text{ s} \left(\frac{10\text{ GeV}}{m_{\chi_1^0}}\right)^5 \left(\frac{m_{3/2}}{100\text{ MeV}}\right)^2\,. \tag{5.2}$$

For light stops, and assuming all other squarks are heavy, the current bounds on the gluino mass are of order TeV. As a possible working example, one can consider $M_{\tilde{g}} \simeq 1.4\,\text{TeV}$, $T_R \simeq 1\,\text{TeV}$, $m_{3/2} \simeq 1\,\text{MeV}$ and neutralino masses of order 40-50 GeV, for which one obtains the proper relic density with a neutralino decaying into gravitinos with a lifetime smaller than a few seconds and therefore not subject to any cosmological or astrophysical constraints.

Another viable candidate for thermal DM in the light neutralino scenario we are considering is the axino $\tilde{a}$, the fermionic supersymmetric partner of the axion $a$. As the MSSM does not provide any solution to the strong CP problem the simplest possibility is to add a (supersymmetrized) axion field, the Goldstone boson of a global PQ symmetry broken at the scale $f_a$ ($5 \times 10^9$ GeV $\lesssim f_a \lesssim 10^{11}$ GeV) that solves dynamically the strong $CP$ problem. Through the supersymmetrization of the anomalous axionic coupling there appears the Lagrangian term [85]

$$\mathcal{L}_{\tilde{a}} = \frac{g'^2 C_a}{32\pi^2 f_a} \bar{\tilde{a}}\gamma_5 \sigma^{\mu\nu} \tilde{B} B_{\mu\nu}\,, \tag{5.3}$$

where $C_a$ is an $\mathcal{O}(1)$ model dependent constant, and which generates in particular the decay $\chi_1^0 \to \tilde{a}\gamma$. Neutralinos should decay at times previous to the nucleosynthesis era not to spoil the BBN predictions. On the other hand, as in the case of gravitino DM, the reheating temperature should be small enough to avoid overproduction but not below the electroweak phase transition temperature to allow the EWBG mechanism to work.



JHEP02(2013)001

The thermal axino relic density is given by [86]

$$\Omega_{\tilde{a}} h^2 \simeq 0.12 \left(\frac{m_{\tilde{a}}}{5\ \text{MeV}}\right) \left(\frac{10^{10}\ \text{GeV}}{f_a}\right)^2 \left(\frac{T_R}{10^3\ \text{GeV}}\right), \tag{5.4}$$

which is normalized to the observed value and shows the range of parameters, $m_{\tilde{a}} \lesssim \text{MeV}$[13] and $T_R \gtrsim \text{TeV}$, leading to the correct relic density. On the other hand the lifetime of neutralinos for the decay channel $\chi_1^0 \to \tilde{a}\gamma$ is given by [85]

$$\tau_{\chi_1^0} \simeq 0.41\,\text{s}\ \frac{1}{C_a^2 N_{11}^2} (128\alpha_{EM})^{-2} \left(\frac{20\ \text{GeV}}{m_{\chi_1^0}}\right)^3 \left(\frac{f_a}{10^{10}\ \text{GeV}}\right)^2, \tag{5.5}$$

where $m_{\tilde{a}} \ll m_{\chi_1^0}$ is assumed and $N_{11}$ is the projection of $\chi_1^0$ along the Bino (for our choice of parameters it is $N_{11} \sim 1$). Then the BBN bound $\tau_{\chi_1^0} \lesssim 1\,s$ is easily evaded for neutralino masses in the ballpark of 20 GeV.

## 6 Conclusions and outlook

In this article we have re-analyzed the LHC constraints on the Light Stop Scenario, a framework of the MSSM where stops lighter than 120 GeV are required by successful EWBG [41, 49]. In this scenario the gluon fusion production rate tends to be enhanced by more than fifty percent with respect to the SM rate, while the width of the Higgs decay into vector gauge bosons, as well as into quarks and leptons, tends to be close to the SM rate. Moreover the Higgs diphoton decay width tends to be somewhat smaller than the SM one.

As previously stated in refs. [52, 53], for $m_h \simeq 125$ GeV there is some tension between the recent Higgs search results at the LHC and the predictions of the Light Stop Scenario, putting strong constraints on the realization of this scenario. These constraints do not only depend on the spectrum of the Light Stop Scenario but also on the specific values of the couplings obtained by requiring EWBG in the MSSM. Taking into account this fact we have found smaller deviations from the Standard Model than those determined in ref. [53]. Moreover we have highlighted that much better agreement with LHC results can be achieved if the lightest neutralino mass is smaller than about 60 GeV. For such light neutralinos the Higgs may have a significant invisible decay width, which may substantially modify the Higgs branching ratios into SM particles.

The precise prediction of the Higgs signatures of the Light Stop Scenario in the presence of light neutralinos does not only depend on the neutralino mass, which is controlled by the bino mass parameter $M_1$, but on $\tan\beta$ and the Higgsino mass parameter $\mu$. Larger values of $\mu$ and/or $\tan\beta$ lead to a suppression of the coupling of the neutralino to the SM-like Higgs and therefore to smaller neutralino effects. Branching ratios of the Higgs decaying into neutralinos of order 30-60% lead to a good agreement of the Light Stop Scenario predictions with the LHC Higgs data. These branching ratios may be obtained for values of the neutralino mass close to $m_h/2$ for low values of $\mu$ and $\tan\beta$ or for larger values of $\mu$ and $\tan\beta$ in the case of light neutralinos, $m_{\chi_1^0} < 45$ GeV.

There are some general features that characterize the proposed scenario:

[13] It has been observed that the axino mass can be hierarchically smaller than the gravitino mass [87].



JHEP02(2013)001

- The Higgs production channels coming from gluon fusion must have enhanced rates with respect to the SM ones.
- The Higgs production channels coming from weak boson fusion must have suppressed rates with respect to the SM ones.
- The $h \to ZZ$ and $h \to WW$ decay rates should be slightly larger than the $h \to \gamma\gamma$ rate in both the gluon fusion and vector boson fusion production channels.
- Apart from a small variation induced by the change in the $h \to \gamma\gamma$ width, for a given Higgs mass the ratios between the different decay channels coming from gluon fusion (or vector boson fusion) are roughly independent of the stop mass and these ratios are not changed by the Higgs decay into neutralinos.

These features are compatible with the present LHC data and they shall be scrutinized with more precise measurements of the Higgs decay rates. In particular, a better understanding of the gluon fusion contribution to the dijet channel is required in order to compare measurements on this process with the vector boson fusion decay $h \to \gamma\gamma$ predicted in the Light Stop Scenario, where the gluon fusion Higgs production is enhanced with respect to the SM one. Due to these unknown systematic uncertainties and lack of statistics, a detailed comparison with LHC data has been left for a future analysis.

Besides the measurements of the visible Higgs decay channels, further issues that we have taken into account in the present analysis are:

- *Higgs invisible width.* The analysis we have performed is very sensitive to this constraint but at present large regions of the parameter space are still allowed. Indeed, current uncertainties on this decay channel are too large to put strong constraints on the model, but in the near future they are expected to substantially decrease.
- *Stop searches.* Light neutralinos can qualitatively modify the stop signatures at LHC. Depending on the neutralino mass the stop is expected to decay into three or four bodies, which finally appear as one jet, one or two leptons and missing energy. Contrarily to what was usually believed for the Light Stop Scenario, these many-body stop decay channels tend to dominate the two-body decay $\tilde{t} \to c\chi_1^0$. The present status of stop searches put constraints that are strongly model dependent and, in general, do not rule out the considered scenario. However dedicated analyses would be worthwhile to probe the existence of light stops and neutralinos, in particular in the presence of light $\tilde{\tau}$'s or $\tilde{\nu}_\tau$'s at the electroweak scale or of several competitive stop decay channels.
- *Z invisible width.* Light neutralinos increase the $Z$ invisible decay width. The SM itself predicts the width of the Z boson into neutrinos to be about one sigma above the LEP measurement. In our analysis we have constrained the $Z$ invisible width to be compatible with the LEP bound at around 95% C.L..

Further phenomenological issues can be considered besides collider physics. The quest for DM candidate is one of them. We have described different solutions to this puzzle



JHEP02(2013)001

within the proposed scenario. For instance if the lightest neutralino is the LSP and has a mass $m_{\chi_1^0} = 35 \div 40\,\text{GeV}$, its thermal relic abundance is mainly determined by its coupling to the $Z$ boson. In part of the parameter space such neutralinos provide the correct DM density, allowing in addition for sufficiently-large Higgs invisible decay. Alternatively, one can also assume that the neutralino is not the LSP. This opens up a wide choice of DM frameworks. For instance, for reheating temperatures of the order of $10 \div 100$ times the electroweak scale, either gravitinos or axinos are plausible DM candidates.

To conclude, the LSS scenario for EWBG in the MSSM is currently being probed at the LHC. Higgs and stop searches are already putting strong constraints on the possible realization of this scenario and more relevant information should be gathered at the end of the present year, when the total integrated luminosity in the most sensitive Higgs search channels will be significantly larger that the present one. More precise data on the Higgs production in the different channels as well as further stop searches at the LHC will be of paramount importance for the ultimate verdict on the feasibility of this scenario.

## Acknowledgments

GN thanks F. Recchia and A. Triossi for programming troubleshooting. MQ was supported in part by the Spanish Consolider-Ingenio 2010 Programme CPAN (CSD2007-00042) and by CICYT-FEDER-FPA2008-01430. Fermilab is operated by Fermi Research Alliance, LLC under Contract No. DE-AC02-07CH11359 with the U.S. Department of Energy. Work at ANL is supported in part by the U.S. Department of Energy (DOE), Div. of HEP, Contract DE-AC02-06CH11357.



## References

[1] A. Sakharov, *Violation of CP invariance, c asymmetry and baryon asymmetry of the universe*, *Pisma Zh. Eksp. Teor. Fiz.* **5** (1967) 32 [INSPIRE].

[2] A.G. Cohen, D. Kaplan and A. Nelson, *Progress in electroweak baryogenesis*, *Ann. Rev. Nucl. Part. Sci.* **43** (1993) 27 [hep-ph/9302210] [INSPIRE].

[3] M. Quirós, *Field theory at finite temperature and phase transitions*, *Helv. Phys. Acta* **67** (1994) 451 [INSPIRE].

[4] M. Quirós, *Finite temperature field theory and phase transitions*, hep-ph/9901312 [INSPIRE].

[5] V. Rubakov and M. Shaposhnikov, *Electroweak baryon number nonconservation in the early universe and in high-energy collisions*, *Usp. Fiz. Nauk* **166** (1996) 493 [hep-ph/9603208] [INSPIRE].

[6] M.S. Carena and C. Wagner, *Electroweak baryogenesis and Higgs physics*, hep-ph/9704347 [INSPIRE].



JHEP02(2013)001

[7] K. Kajantie, K. Rummukainen and M.E. Shaposhnikov, *A lattice Monte Carlo study of the hot electroweak phase transition*, *Nucl. Phys.* **B 407** (1993) 356 [hep-ph/9305345] [INSPIRE].

[8] Z. Fodor, J. Hein, K. Jansen, A. Jaster and I. Montvay, *Simulating the electroweak phase transition in the* SU(2) *Higgs model*, *Nucl. Phys.* **B 439** (1995) 147 [hep-lat/9409017] [INSPIRE].

[9] K. Kajantie, M. Laine, K. Rummukainen and M.E. Shaposhnikov, *The electroweak phase transition: a nonperturbative analysis*, *Nucl. Phys.* **B 466** (1996) 189 [hep-lat/9510020] [INSPIRE].

[10] K. Jansen, *Status of the finite temperature electroweak phase transition on the lattice*, *Nucl. Phys. Proc. Suppl.* **47** (1996) 196 [hep-lat/9509018] [INSPIRE].

[11] G.R. Farrar and M. Shaposhnikov, *Baryon asymmetry of the universe in the minimal standard model*, *Phys. Rev. Lett.* **70** (1993) 2833 [*Erratum ibid.* **71** (1993) 210] [hep-ph/9305274] [INSPIRE].

[12] M. Gavela, P. Hernández, J. Orloff and O. Pene, *Standard model CP-violation and baryon asymmetry*, *Mod. Phys. Lett.* **A 9** (1994) 795 [hep-ph/9312215] [INSPIRE].

[13] M. Gavela, P. Hernández, J. Orloff, O. Pene and C. Quimbay, *Standard model CP-violation and baryon asymmetry. Part 2: finite temperature*, *Nucl. Phys.* **B 430** (1994) 382 [hep-ph/9406289] [INSPIRE].

[14] P. Huet and E. Sather, *Electroweak baryogenesis and standard model CP-violation*, *Phys. Rev.* **D 51** (1995) 379 [hep-ph/9404302] [INSPIRE].

[15] M.S. Carena, M. Quirós and C. Wagner, *Opening the window for electroweak baryogenesis*, *Phys. Lett.* **B 380** (1996) 81 [hep-ph/9603420] [INSPIRE].

[16] D. Delepine, J. Gerard, R. Gonzalez Felipe and J. Weyers, *A light stop and electroweak baryogenesis*, *Phys. Lett.* **B 386** (1996) 183 [hep-ph/9604440] [INSPIRE].

[17] J.M. Cline and K. Kainulainen, *Supersymmetric electroweak phase transition: beyond perturbation theory*, *Nucl. Phys.* **B 482** (1996) 73 [hep-ph/9605235] [INSPIRE].

[18] J.M. Cline and K. Kainulainen, *Supersymmetric electroweak phase transition: dimensional reduction versus effective potential*, *Nucl. Phys.* **B 510** (1998) 88 [hep-ph/9705201] [INSPIRE].

[19] M. Laine and K. Rummukainen, *The MSSM electroweak phase transition on the lattice*, *Nucl. Phys.* **B 535** (1998) 423 [hep-lat/9804019] [INSPIRE].

[20] M. Laine and K. Rummukainen, *A strong electroweak phase transition up to $m_H$ is about* 105 *GeV*, *Phys. Rev. Lett.* **80** (1998) 5259 [hep-ph/9804255] [INSPIRE].

[21] M. Laine, *Effective theories of MSSM at high temperature*, *Nucl. Phys.* **B 481** (1996) 43 [*Erratum ibid.* **B 548** (1999) 637-638] [hep-ph/9605283] [INSPIRE].

[22] M. Losada, *High temperature dimensional reduction of the MSSM and other multiscalar models*, *Phys. Rev.* **D 56** (1997) 2893 [hep-ph/9605266] [INSPIRE].

[23] M. Losada, *The electroweak phase transition in the minimal supersymmetric standard model*, hep-ph/9612337 [INSPIRE].

[24] G.R. Farrar and M. Losada, *SUSY and the electroweak phase transition*, *Phys. Lett.* **B 406** (1997) 60 [hep-ph/9612346] [INSPIRE].

JHEP02(2013)001

[25] J. Espinosa, *Dominant two loop corrections to the MSSM finite temperature effective potential*, *Nucl. Phys.* **B 475** (1996) 273 [hep-ph/9604320] [INSPIRE].

[26] B. de Carlos and J. Espinosa, *The baryogenesis window in the MSSM*, *Nucl. Phys.* **B 503** (1997) 24 [hep-ph/9703212] [INSPIRE].

[27] M.S. Carena, M. Quirós, A. Riotto, I. Vilja and C. Wagner, *Electroweak baryogenesis and low-energy supersymmetry*, *Nucl. Phys.* **B 503** (1997) 387 [hep-ph/9702409] [INSPIRE].

[28] M.S. Carena, M. Quirós and C. Wagner, *Electroweak baryogenesis and Higgs and stop searches at LEP and the Tevatron*, *Nucl. Phys.* **B 524** (1998) 3 [hep-ph/9710401] [INSPIRE].

[29] J.M. Cline, M. Joyce and K. Kainulainen, *Supersymmetric electroweak baryogenesis in the WKB approximation*, *Phys. Lett.* **B 417** (1998) 79 [*Erratum ibid.* **B 448** (1999) 321] [hep-ph/9708393] [INSPIRE].

[30] T. Multamaki and I. Vilja, *CP violation and baryogenesis in the low-energy minimal supersymmetric standard model*, *Phys. Lett.* **B 411** (1997) 301 [hep-ph/9705469] [INSPIRE].

[31] A. Riotto, *More about electroweak baryogenesis in the minimal supersymmetric standard model*, *Int. J. Mod. Phys.* **D 7** (1998) 815 [hep-ph/9709286] [INSPIRE].

[32] M.P. Worah, *Supersymmetric baryogenesis at the electroweak phase transition*, *Phys. Rev.* **D 56** (1997) 2010 [hep-ph/9702423] [INSPIRE].

[33] D. Bödeker, P. John, M. Laine and M. Schmidt, *The two loop MSSM finite temperature effective potential with stop condensation*, *Nucl. Phys.* **B 497** (1997) 387 [hep-ph/9612364] [INSPIRE].

[34] J.M. Cline and G.D. Moore, *Supersymmetric electroweak phase transition: baryogenesis versus experimental constraints*, *Phys. Rev. Lett.* **81** (1998) 3315 [hep-ph/9806354] [INSPIRE].

[35] J.M. Cline and K. Kainulainen, *A new source for electroweak baryogenesis in the MSSM*, *Phys. Rev. Lett.* **85** (2000) 5519 [hep-ph/0002272] [INSPIRE].

[36] J.M. Cline, M. Joyce and K. Kainulainen, *Supersymmetric electroweak baryogenesis*, *JHEP* **07** (2000) 018 [hep-ph/0006119] [INSPIRE].

[37] M.S. Carena, J. Moreno, M. Quirós, M. Seco and C. Wagner, *Supersymmetric CP-violating currents and electroweak baryogenesis*, *Nucl. Phys.* **B 599** (2001) 158 [hep-ph/0011055] [INSPIRE].

[38] M.S. Carena, M. Quirós, M. Seco and C. Wagner, *Improved results in supersymmetric electroweak baryogenesis*, *Nucl. Phys.* **B 650** (2003) 24 [hep-ph/0208043] [INSPIRE].

[39] T. Konstandin, T. Prokopec, M.G. Schmidt and M. Seco, *MSSM electroweak baryogenesis and flavor mixing in transport equations*, *Nucl. Phys.* **B 738** (2006) 1 [hep-ph/0505103] [INSPIRE].

[40] V. Cirigliano, S. Profumo and M.J. Ramsey-Musolf, *Baryogenesis, electric dipole moments and dark matter in the MSSM*, *JHEP* **07** (2006) 002 [hep-ph/0603246] [INSPIRE].

[41] M. Carena, G. Nardini, M. Quirós and C. Wagner, *The baryogenesis window in the MSSM*, *Nucl. Phys.* **B 812** (2009) 243 [arXiv:0809.3760] [INSPIRE].

[42] ATLAS collaboration, *Observation of an excess of events in the search for the standard model Higgs boson with the ATLAS detector at the LHC*, ATLAS-CONF-2012-093 (2012).



JHEP02(2013)001

[43] J. Incandela, *Update on the standard model Higgs searches in CMS*, CERN Seminar, July 4, 2012.

[44] ATLAS collaboration, *Search for the standard model Higgs boson in the diphoton decay channel with 4.9 fb$^{-1}$ of pp collisions at $\sqrt{s} = 7$ TeV with ATLAS*, *Phys. Rev. Lett.* **108** (2012) 111803 [arXiv:1202.1414] [INSPIRE].

[45] CMS collaboration, *Search for the standard model Higgs boson decaying into two photons in pp collisions at $\sqrt{s} = 7$ TeV*, *Phys. Lett.* **B 710** (2012) 403 [arXiv:1202.1487] [INSPIRE].

[46] ATLAS collaboration, *Observation of an excess of events in the search for the standard model Higgs boson in the $\gamma$-$\gamma$ channel with the ATLAS detector*, ATLAS-CONF-2012-091 (2012).

[47] CMS collaboration, *Evidence for a new state decaying into two photons in the search for the standard model Higgs boson in pp collisions*, HIG-12-015 (2012).

[48] O. Arnaez, *Searches for the SM scalar boson in the WW decay channel with the ATLAS experiment*, talk given at the *Higgs Hunting 2012 Conference*, Orsay, France, July 18, 2012.

[49] M. Carena, G. Nardini, M. Quirós and C.E. Wagner, *The effective theory of the light stop scenario*, *JHEP* **10** (2008) 062 [arXiv:0806.4297] [INSPIRE].

[50] A. Djouadi, *The anatomy of electro-weak symmetry breaking. II. The Higgs bosons in the minimal supersymmetric model*, *Phys. Rept.* **459** (2008) 1 [hep-ph/0503173] [INSPIRE].

[51] A. Menon and D.E. Morrissey, *Higgs boson signatures of MSSM electroweak baryogenesis*, *Phys. Rev.* **D 79** (2009) 115020 [arXiv:0903.3038] [INSPIRE].

[52] T. Cohen, D.E. Morrissey and A. Pierce, *Electroweak baryogenesis and Higgs signatures*, *Phys. Rev.* **D 86** (2012) 013009 [arXiv:1203.2924] [INSPIRE].

[53] D. Curtin, P. Jaiswal and P. Meade, *Excluding electroweak baryogenesis in the MSSM*, *JHEP* **08** (2012) 005 [arXiv:1203.2932] [INSPIRE].

[54] A. Delgado, G. Nardini and M. Quirós, *The light stop scenario from gauge mediation*, *JHEP* **04** (2012) 137 [arXiv:1201.5164] [INSPIRE].

[55] R. Essig, E. Izaguirre, J. Kaplan and J.G. Wacker, *Heavy flavor simplified models at the LHC*, *JHEP* **01** (2012) 074 [arXiv:1110.6443] [INSPIRE].

[56] Y. Kats, P. Meade, M. Reece and D. Shih, *The status of GMSB after 1/fb at the LHC*, *JHEP* **02** (2012) 115 [arXiv:1110.6444] [INSPIRE].

[57] M. Papucci, J.T. Ruderman and A. Weiler, *Natural SUSY endures*, *JHEP* **09** (2012) 035 [arXiv:1110.6926] [INSPIRE].

[58] X.-J. Bi, Q.-S. Yan and P.-F. Yin, *Probing light stop pairs at the LHC*, *Phys. Rev.* **D 85** (2012) 035005 [arXiv:1111.2250] [INSPIRE].

[59] C. Brust, A. Katz, S. Lawrence and R. Sundrum, *SUSY, the third generation and the LHC*, *JHEP* **03** (2012) 103 [arXiv:1110.6670] [INSPIRE].

[60] N. Desai and B. Mukhopadhyaya, *Constraints on supersymmetry with light third family from LHC data*, *JHEP* **05** (2012) 057 [arXiv:1111.2830] [INSPIRE].

[61] A. Choudhury and A. Datta, *New limits on top squark NLSP from LHC 4.7 fb$^{-1}$ data*, *Mod. Phys. Lett.* **A 27** (2012) 1250188 [arXiv:1207.1846] [INSPIRE].

JHEP02(2013)001

[62] CDF collaboration, T. Aaltonen et al., *Search for pair production of supersymmetric top quarks in dilepton events from $p\bar{p}$ collisions at $\sqrt{s} = 1.96$ TeV*, *Phys. Rev. Lett.* **104** (2010) 251801 [arXiv:0912.1308] [INSPIRE].

[63] ATLAS collaboration, *Search for light scalar top quark pair production in final states with two leptons with the ATLAS detector in $\sqrt{s} = 7$ TeV proton-proton collisions*, *Eur. Phys. J.* **C 72** (2012) 2237 [arXiv:1208.4305] [INSPIRE].

[64] ATLAS collaboration, *Search for light top squark pair production in final states with leptons and b-jets with the ATLAS detector in $\sqrt{s} = 7$ TeV proton-proton collisions*, ATLAS-CONF-2012-070 (2012).

[65] ATLAS collaboration, *Search for light top squark pair production in final states with leptons and b-jets with the ATLAS detector in $\sqrt{s} = 7$ TeV proton-proton collisions*, ATLAS-CONF-2012-070 (2012).

[66] CDF AND D0 collaborations, P. Calfayan, *Search for scalar top and bottom quarks at the Tevatron*, *AIP Conf. Proc.* **1078** (2009) 262 [INSPIRE].

[67] M. Carena, S. Gori, N.R. Shah and C.E. Wagner, *A 125 GeV SM-like Higgs in the MSSM and the $\gamma\gamma$ rate*, *JHEP* **03** (2012) 014 [arXiv:1112.3336] [INSPIRE].

[68] M. Carena, S. Gori, N.R. Shah, C.E. Wagner and L.-T. Wang, *Light Stau phenomenology and the Higgs $\gamma\gamma$ rate*, *JHEP* **07** (2012) 175 [arXiv:1205.5842] [INSPIRE].

[69] J. Kozaczuk, S. Profumo, M.J. Ramsey-Musolf and C.L. Wainwright, *Supersymmetric electroweak baryogenesis via resonant sfermion sources*, *Phys. Rev.* **D 86** (2012) 096001 [arXiv:1206.4100] [INSPIRE].

[70] ALEPH collaboration, A. Heister et al., *Search for scalar quarks in $e^+e^-$ collisions at $\sqrt{s}$ up to 209 GeV*, *Phys. Lett.* **B 537** (2002) 5 [hep-ex/0204036] [INSPIRE].

[71] K.-i. Hikasa and M. Kobayashi, *Light scalar top at $e^+e^-$ colliders*, *Phys. Rev.* **D 36** (1987) 724 [INSPIRE].

[72] C. Boehm, A. Djouadi and Y. Mambrini, *Decays of the lightest top squark*, *Phys. Rev.* **D 61** (2000) 095006 [hep-ph/9907428] [INSPIRE].

[73] M. Muhlleitner and E. Popenda, *Light stop decay in the MSSM with minimal flavour violation*, *JHEP* **04** (2011) 095 [arXiv:1102.5712] [INSPIRE].

[74] M. Hosch, R. Oakes, K. Whisnant, J.M. Yang, B.-l. Young, et al., *Probing top quark decay into light stop in the supersymmetric standard model at the upgraded Tevatron*, *Phys. Rev.* **D 58** (1998) 034002 [hep-ph/9711234] [INSPIRE].

[75] CDF COLLABORATION, D0 collaboration, V. Shary, *Studies of top quark properties at the Tevatron*, arXiv:1205.3771 [INSPIRE].

[76] PARTICLE DATA GROUP collaboration, K. Nakamura et al., *Review of particle physics*, *J. Phys.* **G 37** (2010) 075021 [INSPIRE].

[77] H.K. Dreiner, S. Heinemeyer, O. Kittel, U. Langenfeld, A.M. Weber, et al., *Mass bounds on a very light neutralino*, *Eur. Phys. J.* **C 62** (2009) 547 [arXiv:0901.3485] [INSPIRE].

[78] ATLAS collaboration, *Search for new phenomena in monojet plus missing transverse momentum final states using 1 $fb^{-1}$ of pp collisions at $\sqrt{s} = 7$ TeV with the ATLAS detector*, ATLAS-CONF-2011-096 (2011).

JHEP02(2013)001

[79] C. Englert, J. Jaeckel, E. Re and M. Spannowsky, *Evasive Higgs maneuvers at the LHC*, *Phys. Rev.* **D 85** (2012) 035008 [arXiv:1111.1719] [INSPIRE].

[80] Y. Bai, P. Draper and J. Shelton, *Measuring the invisible Higgs width at the 7 and 8 TeV LHC*, *JHEP* **07** (2012) 192 [arXiv:1112.4496] [INSPIRE].

[81] A. Djouadi, A. Falkowski, Y. Mambrini and J. Quevillon, *Direct detection of Higgs-portal dark matter at the LHC*, arXiv:1205.3169 [INSPIRE].

[82] ATLAS collaboration, *Coupling properties of the new Higgs-like boson observed with the ATLAS detector at the LHC*, ATLAS-CONF-2012-127 (2012).

[83] A. Menon, D. Morrissey and C. Wagner, *Electroweak baryogenesis and dark matter in the NMSSM*, *Phys. Rev.* **D 70** (2004) 035005 [hep-ph/0404184] [INSPIRE].

[84] J. Pradler and F.D. Steffen, *Constraints on the reheating temperature in gravitino dark matter scenarios*, *Phys. Lett.* **B 648** (2007) 224 [hep-ph/0612291] [INSPIRE].

[85] L. Covi, H.-B. Kim, J.E. Kim and L. Roszkowski, *Axinos as dark matter*, *JHEP* **05** (2001) 033 [hep-ph/0101009] [INSPIRE].

[86] A. Brandenburg and F.D. Steffen, *Axino dark matter from thermal production*, *JCAP* **08** (2004) 008 [hep-ph/0405158] [INSPIRE].

[87] E. Chun, J.E. Kim and H.P. Nilles, *Axino mass*, *Phys. Lett.* **B 287** (1992) 123 [hep-ph/9205229] [INSPIRE].

JHEP02(2013)001